

Article

Remote Sensing-Based Assessment of the Variability of Winter and Summer Precipitation in the Pamirs and Their Effects on Hydrology and Hazards Using Harmonic Time Series Analysis

Eric Pohl ^{1,*}, Richard Gloaguen ^{1,2} and Ralf Seiler ¹

¹ Remote Sensing Group, Institute of Geology, Technische Universität Bergakademie Freiberg, B.-von-Cotta-Str. 2, Freiberg D-09599, Germany; E-Mails: r.gloaguen@hzdr.de (R.G.); r.seiler@r6s-consult.de (R.S.)

² Remote Sensing Group, Helmholtz Institute Freiberg for Resource Technology, Freiberg D-09599, Germany

* Author to whom correspondence should be addressed; E-Mail: Eric.Pohl@geo.tu-freiberg.de; Tel.: +49-3731-393-058.

Academic Editors: Assefa M. Melesse, George P. Petropoulos and Prasad S. Thenkabail

Received: 19 February 2015 / Accepted: 21 July 2015 / Published: 30 July 2015

Abstract: Moisture supply in the Pamir Mountains of Central Asia significantly determines the hydrological cycle and, as a result, impacts the local communities via hazards or socioeconomic aspects, such as hydropower, agriculture and infrastructure. Scarce and unreliable *in situ* data prevent an accurate assessment of moisture supply, as well as its temporal and spatial variability in this strongly-heterogeneous environment. On the other hand, a clear understanding of climatic and surface processes is required in order to assess water resources and natural hazards. We propose to evaluate the potential of remote sensing and regional climate model (RCM) data to overcome such issues. Difficulties arise for the direct analysis of precipitation if the events are sporadic and when the amounts are low. We hence apply a harmonic time series analysis (HANTS) algorithm to derive spatio-temporal precipitation distributions and to determine regional boundaries delimiting areas where winter or summer precipitation dominate moisture supply. We complement the study with remote sensing-based products, such as temperature, snow cover and liquid water equivalent thickness. We find a strong intra- and inter-annual variability of meteorological parameters that result in strongly variable water budget and water mobilization. Climatic variability and its effects on floods and droughts are discussed for three outstanding years. The in-house

developed HANTS toolbox is a promising instrument to unravel periodic signals in remote sensing time series, even in complex areas, such as the Pamir.

Keywords: Westerlies; Indian summer monsoon; weather/climate variability; hydrology; hazards

1. Introduction

Central Asia's mountain ranges act as water towers for downstream regions by intercepting moisture transported by the eastward Westerlies and the northward Indian summer monsoon [1–3]. This general characterization has been addressed to precisely point out underlying circulation mechanisms [4], but the interaction of summer and winter circulations on moisture transport are still relatively unconstrained. The largest portion of moisture is provided as snow [1,5], which, when melted during summer, feed the Central Asian rivers. Moreover, snow precipitation provide moisture to glaciers, which represent the most important source of river discharge during late summer [1,6–8]. Despite such relevance, quantifying the actual moisture supply and obtaining systematic precipitation distributions remains a major challenge. Various studies dealt with this issue by assessing rain/snow gauges, remote sensing and climate model data (e.g., [5,9,10]). However, the lack of a dense gauging network, the inability of remote sensing instruments to detect snowfall over persisting snow cover [11,12] and the huge variances in climate model data result in substantial qualitative uncertainties in where and how much precipitation is actually provided [1,10].

Studies based on hydrological modeling are able to validate precipitation quantities by comparing modeled snow and glacier melt amounts with observed discharge. This attempt is prone to errors due to the high impact of glacier melts in the hydrological budget [1,6,8], because adapting glacier melt [1], a quantity that is even less restricted than precipitation amounts, due to an even sparser measuring network [8,13], may allow the compensation of wrongly-assessed precipitation amounts. The reconstruction of the paleoclimate based on past glacier retreats and advances [14–16] is even more challenging, as boundary conditions, such as insolation, temperature, weakening of synoptic scale circulations and timing of precipitation, are less constrained than they are today. These high uncertainties often lead to simplified interpretations, such as generally intensified Westerlies or Indian summer monsoon (ISM) [14–16].

These uncertainties demand for alternative approaches to constrain the sphere of influence of the Westerlies and the ISM in the Pamirs or, more generally speaking, the influences of summer and winter precipitation. While there is consensus of the transition from more summer to winter precipitation-dominated regions from the Himalayas to the Pamirs [5,9,10,17], it remains unclear if this transition has a sharp boundary or if there is a smooth gradient. Maussion *et al.* [17] have delineated seasonal figures that already indicated such regions, showing that winter precipitation dominates far into the Karakoram region. This is especially interesting with respect to contrasting reports of positive and negative glacier mass balances across the Pamirs (Gardelle *et al.* [18] and Gardelle *et al.* [19]; *cf.* Sorg *et al.* [8] and Unger-Shayesteh *et al.* [13]), which might be related to yet unresolved local-scale

climate variations or even unresolved precipitation occurrence in general. The impact of onset timing of the ISM on Tibetan glacier evolution [20] raises the question if a likewise dependency is effecting glacier evolution in the Pamirs. However, Mölg *et al.* [20] also point out that local- or regional-scale circulations rather than synoptic-scale climate is the important key aspect to describe glacier dynamics. This demands for a sufficiently spatially-resolved analysis.

Global climate models (GCM) often have resolutions in several tens to hundreds of km² spatially and, hence, are unemployable to resolve local- and regional-scale characteristics, thus leading to weak correlation with *in situ* data. Regional climate models (RCM) and remote sensing data provide much better resolutions. The RCM HAR10 (10-km resolution High Asia Reanalysis) [17], for example, shows a high correlation with *in situ* precipitation measurements in the Gunt catchment in the Central Pamirs [1], although overestimating actual precipitation amounts. A major drawback of such high-resolution datasets is the often limited time span for which these data are available (12 years for HAR10). The analysis of precipitation time series is even more challenging if there is no pronounced seasonality and high intra-annual variation. A promising and steadily improving method to overcome such issues is the harmonic time series analysis (HANTS) [21,22] that is used to analyze a variety of natural phenomenon, such as phenology (e.g., [21,22]), diurnal precipitation distributions [23], air temperatures [24] or land surface temperatures [25]. Several studies already explored the application of harmonic analysis, showing its potential to reveal precipitation seasonalities [26–29]. The previously developed, open access toolbox for HANTS analysis “phenotemp” [30,31] provides a collection of different HANTS methods for such analyses.

We propose to use remote sensing data products to estimate the spatiotemporal variability of some climatic indicators in the region. As water availability seems one of the major parameters affecting the climatic conditions in the orogen, we focus on HANTS to explore the inter-annual variability of precipitation in the Pamir region. Specifically, this paper addresses the following issues: (1) determination of the spatiotemporal influence of winter and summer precipitation in the Pamirs; (2) to support the analysis of precipitation time series, we incorporate snow cover, temperature and water storage data to reveal interrelations with precipitation and to independently validate the inferences based on the HANTS of precipitation; (3) we relate the obtained results to recent glacier evolution, to point out possible key mechanisms related to weather variability; and (4) we compare exceptional meteorological/weather conditions with the occurrence of regional-scale hazard events, including floods and droughts in the first decade of the 21st century in the greater Pamir region to point out possible causalities.

2. Study Area

The Pamirs mark the transition zone between the Westerlies and the Indian summer monsoon, but several additional mesoscale circulation systems [4] increase the complexity of this binomial delineation. Complex terrain with strongly incised geomorphology on the Pamir margins and a low relief, high altitude plateau in the central Pamirs further highlight that the Pamirs include a more diverse meteorological setting. Westerly winds are deflected to the north and south during winter and provide precipitation mainly as snow to the Pamir margins [5,32]. Precipitation records of few existing

meteorological stations show a minor, but noticeable amount of summer precipitation in the eastern central Pamir region [1]. Precise information is rare about the actual precipitation distribution due to the lack of a dense gauging network. Different studies comfort the assumption that the region receives variable amounts of precipitation with a decreasing W-E trend [1,8,33]. We hence divide the greater Pamir region (Figure 1) into seven subregions bounded by notable orographic barriers and name them based on dominant mountain systems.

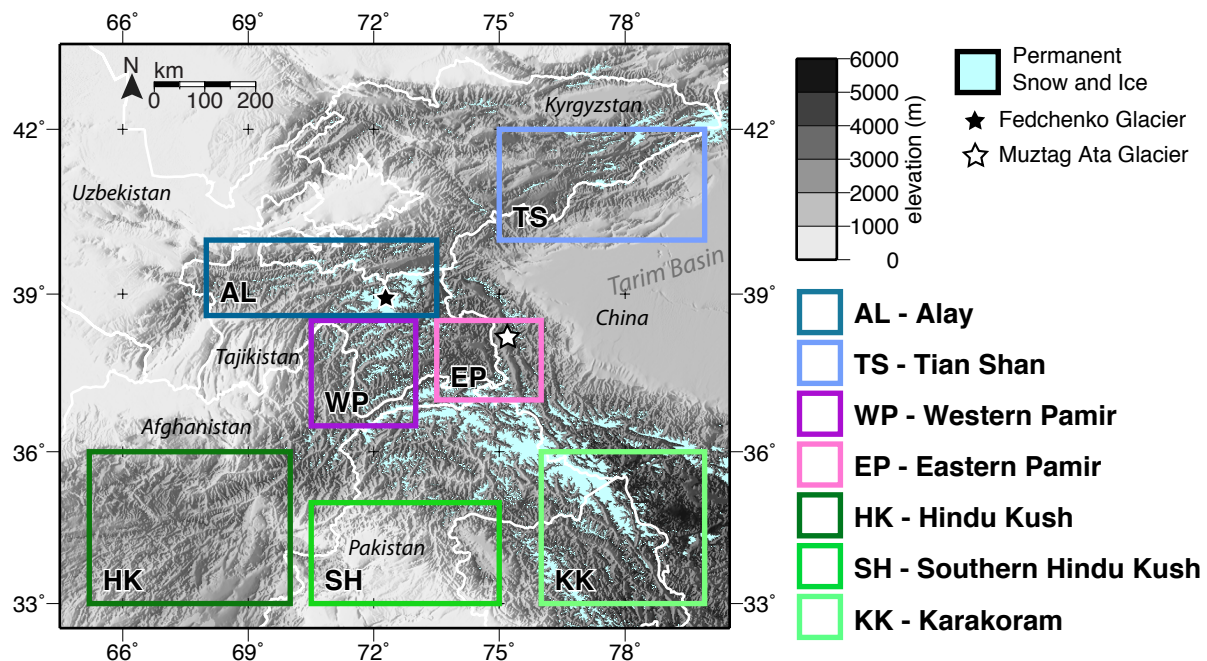


Figure 1. Study area with selected subdivided study sites. Glacier extent is approximated from MODIS MCD12Q1 land cover. Subdivided study sites were defined based on expected precipitation regimes and are named based on the dominant surrounding mountain system.

The subregions Alay Mountains (AL) and Tian Shan (TS) in the northern part mark the outermost orographic barrier that would intercept southward moisture supply. In the central part, the Western Pamir (WP) would intercept direct westward moisture supply, while the Eastern Pamir (EP) lies in the orographic precipitation shadow and is assumed to generally receive very little precipitation, but might have a dominant summer influence [1]. The Western Hindu Kush (HK) is assumed to intercept the southward deflection of westerly winds mainly during winter and might also act as a barrier for far-reaching ISM extensions that are assumed to be most dominant in the lowlands in the Southern Hindu Kush (SH). The Karakoram Range (KK) receives much snowfall, probably related to westerly extensions [5], but since it is located even more eastwards than SH, a noticeable ISM influence is assumed.

3. Data

In order to relate the precipitation analysis to a broader context in terms of hydrology, meteorology and hazards, we incorporate temperature, snow cover and liquid water equivalent thickness (LWET) data. Ideally, we would have selected only remote sensing products for this study. Pohl *et al.* [1]

and Palazzi *et al.* [10] have shown that state-of-the-art precipitation datasets for the Pamir region show big differences, both in intensity and spatial distribution. In a previous work [1], we tested different precipitation products for their application in a hydrological modeling approach in the Pamir Mountains. We found that the frequently-used TRMM (Tropical Rainfall Measuring Mission) 3B42 V7 dataset [34–36] most likely suffers from issues with snowfall determination [11,37–39]. Even though the used microwave imagers can recognize snowfall, the quality relies on the discrimination between frozen precipitation and antecedent snow cover [11]. Kamal-Heikman *et al.* [38] also reported an underestimation of precipitation in cases of intense snowfall in the Himalayas. We found that the RCM dataset HAR (High Asia Reanalysis) [17] provides the most reliable estimates for precipitation in the Central Pamirs. However, good correlation with *in situ* measurements contrasts an overestimation of actual precipitation amounts. The reported overestimation is consistent for low and high elevation pixels, hence the required spatial patterns, and event timings are not affected by a lack of calibration.

The relatively short time spans of the used meteorological data (≈ 12 years) does not allow a full analysis in a climatological context. However, comparison of obtained HANTS results for the timing of winter and summer precipitation is in strong agreement with ECMWF (European Centre for Medium-Range Weather Forecasts) ERA-Interim data [40] that span a 35-year period (Figure 8). For the meteorological parameters snow cover, temperature and LWET, we do not apply the HANTS algorithm, because these parameters already show very continuous signals that allow analysis based on long-term means and corresponding anomalies for individual periods (monthly, winter, summer).

HAR results from a dynamical downscaling of global analysis data (final analysis data from the Global Forecasting System [41]; dataset ds083.2) using the Weather Research and Forecasting (WRF) model [42]. HAR data are available from 2001 to 2012 at different spatial extents and spatial resolutions. We used the 30-km resolution HAR30 dataset that fully covers the study area. We further use HAR30 2-m air temperature data that result from the same modeling. Pohl *et al.* [1] have validated the finer resolution HAR10 (10-km resolution) datasets in the central Pamirs. Because HAR10 does not spatially cover the study region, we use the HAR30 dataset, which is consistent with the 10-km resolution version. Although HAR is a modeled and not a directly-derived remote sensing dataset, it comprises the same structure as other remote sensing data products. The applied method in this study, therefore, suits the application to other precipitation datasets, where those data provide reliable estimates.

To evaluate whether precipitation falls as snow or rain, we use the MODIS (Moderate-Resolution Imaging Spectroradiometer) MOD10CM [43] monthly snow cover dataset. We use the time span from January 2001 until December 2012 to match the period available for HAR. This dataset comes originally in a spatial resolution of 0.05° and was resampled using mean values to $\approx 0.3^\circ$ to allow for faster processing and to match the resolution of the precipitation and temperature datasets. MODIS snow cover data are very frequently used for hydrological and climate change scenario studies [3,5,44]. MOD10CM is an averaged monthly product based on the daily MODIS MOD10C1 [45] product.

To evaluate meteorological influences on the water balance of the regions, we use the GRACE (Gravity Recovery and Climate Experiment) [46,47] dataset GFZ (German Research Centre for Geosciences) release RL05 [48]. GFZ RL05 is available from 2003 to 2012 in monthly temporal and $1 \times 1^\circ$ spatial resolution. GRACE measures the Earth's gravity field and its time variability. The major influence on time variability is the amount of stored water, and hence, variations in observed gravity

can be used as a proxy for liquid water equivalent thickness (LWET). We use the GFZ RL05 dataset in this study to highlight the influences of meteorological configurations on the regional hydrological water budget. Several hydrological studies make use of GRACE data to access monthly changes in the water balance [49–51], but GRACE data have also been utilized to assess regional and global glacier mass balance changes [51,52].

Table 1. Selected hazard events from Emergency Events Database (EM-DAT) [53] in the greater Pamir region and adjacent regions for the years 2005, 2008 and 2010. Events are listed according to affected country, rather than exact locations. AF, Afghanistan; PK, Pakistan; TJ, Tajikistan; KY, Kyrgyzstan; UZ, Uzbekistan.

Country	Event Type	Date	People Affected
2005			
AF	Storm	January 2005	22,656
AF	Flood	05 March 2005	11003
AF	Flood	16 June 2005	5040
PK	Flood	09 February 2005	7,000,450
PK	Flood	21 June 2005	460,073
PK	Flood	05 July 2005	58,020
PK	Flood	02 March 2005	5000
PK	Flood	20 March 2005	3500
TJ	Flood	08 June 2005	3222
TJ	Mass movement wet	03 February 2005	1953
TJ	Flood	23 July 2005	1890
KY	Flood	10 June 2005	2050
UZ	Flood	24 February 2005	1500
2008			
AF	Drought	October 2008	280,000
AF	Flood	August 2008	1180
PK	Flood	02 August 2008	200,012
PK	Flood	09 August 2008	90,752
TJ	Drought	October 2008	800,000
2010			
AF	Flood	05 May 2010	40,000
AF	Flood	27 July 2010	5000
PK	Flood	28 July 2010	20,359,496
PK	Mass Movement Wet	04 January 2010	26,700
PK	Storm	06 June 2010	4000
PK	Flood	21 July 2010	4000
PK	Mass Movement Wet	18 February 2010	3705
TJ	Flood	06 May 2010	6708
TJ	Flood	11 April 2010	1914
KY	Mass Movement Wet	03 June 2010	8350

We further use the Emergency Events Database (EM-DAT) of the Centre for Research on the Epidemiology of Disasters (CRED) [53] to qualitatively relate the meteorological interplay with hazard events. Assessing hazards is always coupled to the effect an event, such as a flood, mudflow or avalanche, has on local communities. It is hence difficult to localize the exact extent or area of influence of such events if very few people or little infrastructure is affected. The needed detailed analysis of appropriate imagery data would go beyond the scope of this work. Hence, we use EM-DAT events that have at least 100 people affected (see <http://www.emdat.be/explanatory-notes> for the full list of criteria). EM-DAT does not claim completeness, but lists the major events and, thus, provides event records for the entire study period and lists major events by country. Selected events are summarized in Table 1. The fact that events are stated by country prevents a local-scale analysis. However, in the case of droughts and severe floods, large proportions of the river catchments can be assumed to play an important role. This is because the main rivers in the study area originate in the high mountains and are affected by the regional meteorological conditions in the orogen. We want to point out that we do not intend to provide a local hazard assessment in this study. We rather want to demonstrate whether large-scale climatic events coincide with large-scale hazards and discuss a probable causal relationship.

4. Methods

Precipitation occurs as discrete events, *i.e.*, it takes place during a day or over a few days with intermediate gaps. Even in regions influenced by monsoon, there is no continuous signal of precipitation. In the Pamirs, most precipitation occurs during winter and early spring with a strong decreasing W-E gradient [1,2]. As a result, precipitation amounts and intensities are generally low, and it is difficult to derive seasonal patterns based on ordinary moving averages (Figure 2a). Few precipitation events further complicate the determination of the timing of when an individual season peaks. To overcome this issue, we apply the HANTS algorithm [21,22].

4.1. HANTS

The aim of HANTS as presented by Roerink *et al.* [22] and de Jong *et al.* [21] is to remove pixel-wise cloud-affected observations and to temporally interpolate a given time series of remote sensing vegetation data. HANTS is a multi-step approach that in the end represents a given time series by means of a limited amount of cosine functions with different phases, frequencies and amplitudes [21]. In the first step, the Fourier series are calculated. Depending on the assumed number of harmonic signals, e.g., annual, seasonal, *etc.*, a corresponding number of Fourier series with according frequencies are calculated. Each data point of the original time series is replaced by the (smoothed) value of the combined Fourier series, if its residual is above a manually set threshold. Once this replacement has been done for all points of the time series, the algorithm checks whether (1) a predefined number of iterations have been calculated or (2) an also *a priori*-specified max percentage of data points has been changed from the original to a smoothed value. If one of the two criteria is met, the algorithm terminates. Otherwise, it starts a new iteration with calculating the set of Fourier series from the now partially-smoothed data. Seiler [30], and Seiler and Gloaguen [31] developed a standalone, open access Java application “phenotemp”, which provides a compilation of different modifications of HANTS, of

which the version after de Jong *et al.* [21] was used in this study. We used phenotemp to obtain (1) the average annual pattern (based on the full time series) and (2) the individual annual patterns (Figure 2b).

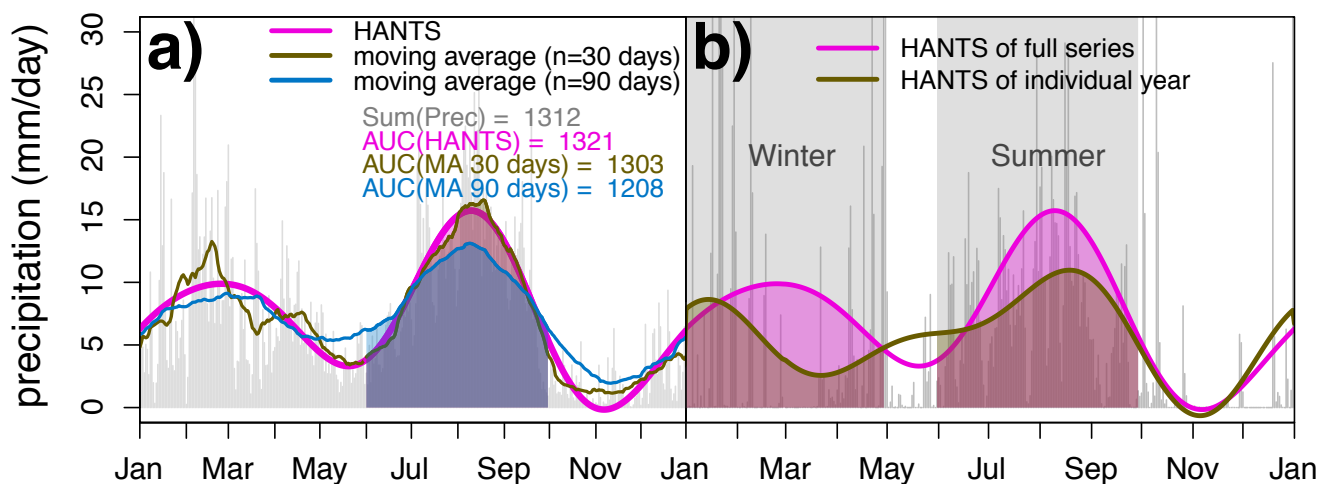


Figure 2. Harmonic time series analysis (HANTS) principals. (a) HANTS vs. running means with different window widths applied to a precipitation time series (grey) of a randomly-selected pixel; (b) HANTS is applied to find the maximum of the full time series and of individual years to determine the peak precipitation timing for each pixel (see Section 5). Anomalies are calculated as the difference of the area under the curve (AUC) of either the winter or summer season of an individual year and the full time series. Note that “HANTS of full series” is calculated based on the full length of the time series and shows the same shape in every year. “HANTS of individual year” is calculated individually for each year of the full time series, and thus, its curves show different shapes from year to year. Here, only one year is displayed for the sake of brevity.

Differences between the integrals of the average and individual years are calculated as winter (JFMA; January–April) and summer (JJAS; June–September) anomalies. The algorithm needs three parameters: (1) the maximum number of iterations *maxIt*; (2) the maximum tolerance of original data points from the smoothed time series *maxTol*; and (3) the minimum number of preserved data points *minPres*. HANTS lacks an objective rule to set these parameters [21]. Because we intend to unambiguously determine HANTS maxima, we set *maxTol* = 0, which preserves a continuous HANTS signal (*maxTol* > 0 can result in several maxima, as is the case for moving averages; see Figure 2a). *maxIt* and *minPres* were set to 10 times and 67%, respectively. We have tested the HANTS algorithm on three *in situ* precipitation time series in the Central Pamirs that show different intensities and seasonalities. In either case, HANTS was able to precisely represent the long-term average annual cyclicity and intensities. This ability has been utilized by other studies to identify precipitation seasonalities and the influences of synoptic and regional-scale atmospheric circulations on the distribution of precipitation [28,29].

The application of HANTS comprises noticeable additional effort in comparison to the application of, e.g., moving averages (MA). Therefore, we summarize some major issues that can result from the application of moving averages and why HANTS provides an advantage in particular cases. The example provided in Figure 3 shows a synthetic precipitation time series with a bi-modal peak that can be expected in the transition zone between winter and summer precipitation-dominated regions. The basis of the time

series is a combined sine function with distinct frequencies of 2π and 4π , respectively. Noise was added by means of uniformly-distributed values and by randomly removing data points. This was done to test both MA's and HANTS' ability to reveal the underlying periodic signal. The calculation of mean daily values, followed by an application of MA, is able to identify the timing of the peak amplitude of the underlying signal if the time series is long enough or the average signal is pronounced enough (Figure 3c).

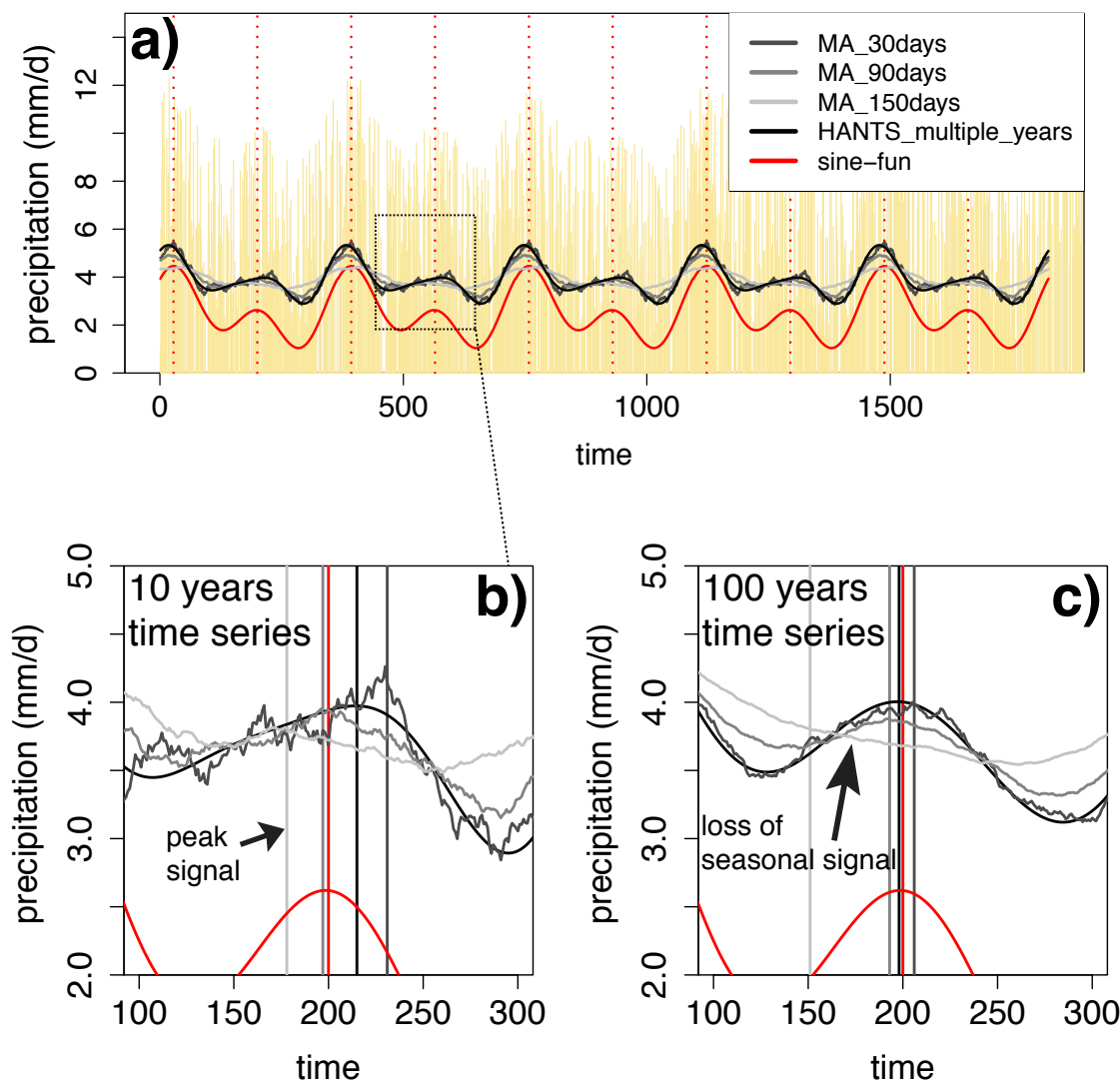


Figure 3. Comparison of HANTS and moving averages (MA). (a) Synthetic time series of precipitation data (yellow) based on two added sine functions with frequencies of 2π and 4π per year and a phase offset to model a signal similar to possible bi-modal curves with a winter and a summer peak (red curve). Noise added by (1) means of a uniform distribution with values between 0 and 8 and (2) additional random removal of individual values. (b) Different MA with varying window sizes applied to mean daily values of the generated time series with a 10-year period. Displayed HANTS (“full series”) is based on the same time series. (c) Same as for (b), but based on time series of 100 years. Vertical bars indicate the maximum of individual curves within a 100-day window around the actual maxima of the original overlain sine functions.

Based on the choice of the moving window, the results are not as distinct. In particular, the choice of the moving window affects the determination of the real underlying seasonal patterns. Small window sizes are sensitive to fluctuations (Figure 3b; 30-day window size) and might introduce temporal bias, and windows that are too long might result in the diminution of the seasonal signal (Figure 3c; 150-day window size). The presented HANTS in this study, by definition, does not allow high frequency fluctuations, but preserves a continuous signal, nor does its application dampen (or even remove) the amplitude of the signal, which is the case for MA with a large window sizes. As shown in Figure 2, the dampening of the signal amplitude from MA with a large window size will lead to a biased assessment of AUC. This bias prevents meaningful quantitative analysis. In summary, HANTS combines the robustness of MA with large window sizes to reveal low-frequency seasonal signals and the ability of MA with small window sizes to preserve amplitudes of seasonal signals. HANTS series are better at preserving the real times of maxima and the original signal intensity.

5. Results

The greater Pamir region encompasses complex topographic and climatic settings, which prevent a simple spatiotemporal classification. Instead of trying to describe all of the processes and their interactions, we present the general patterns of precipitation intensities and timing (Figures 4 and 5). In order to display the temporal dynamics, we present regionally-averaged time series for individual regions, which we have described in Section 2. This step is required due to the large amount of spatiotemporal data that would exceed the scope of this article by far. However, the simplification by means of regional averaged time series hampers the identification of the associated spatial patterns. Therefore, we highlight three individual years that show the outstanding interplay of meteorological parameters and specific effects on LWET (Figure 6) in Section 5.2.

5.1. Mean Patterns and Inter-Annual Variability

There are strong differences in the average winter and summer precipitation distribution (Figure 4). Most significant amounts in winter are provided to the western sites AL and WP, but also to the northern Hindu Kush and to the northern Karakoram Range (Figure 4b). In contrast, the HK site and the lowlands in SH, as well as TS receive very little precipitation. In summer, significant amounts are provided to TS, EP and SH (Figure 4c). The WP and HK receive almost no precipitation in summer.

The maxima of the HANTS analysis for the full time series (Figure 5) show similar timings of peak precipitation for the HAR30 (Figure 5a) precipitation dataset (12 years) and ERA-Interim (Figure 5b) (35 years). The higher spatial resolution of HAR30 discriminates regions that are entirely winter-/summer-dominated and regions showing partial domination. Entirely winter-dominated are HK and WP, while TS and the southern part of SH, *i.e.*, the lowlands, are summer-dominated. Striking is a sharp discrimination of either winter- or summer-domination in the SH and KK, but also the EP site. In contrast to these sharp differences, there are several transitional regions that show successive temporal gradients of peak precipitation input. Most pronounced here is the AL region with a W-E gradient of later peak precipitation occurrence. Similarly, the entire Tarim Basin shows smooth transitional timings. While TS shows a distinct summer peak, northward and southward timings are successively earlier.

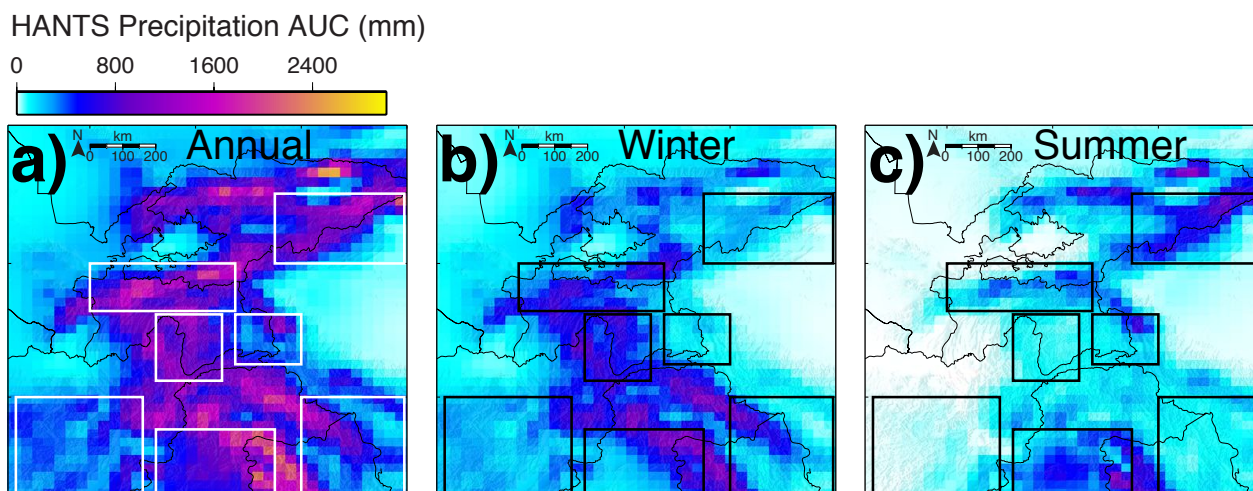


Figure 4. Precipitation distributions of the applied HANTS method for the (a) annual, (b) winter and (c) summer precipitation patterns.

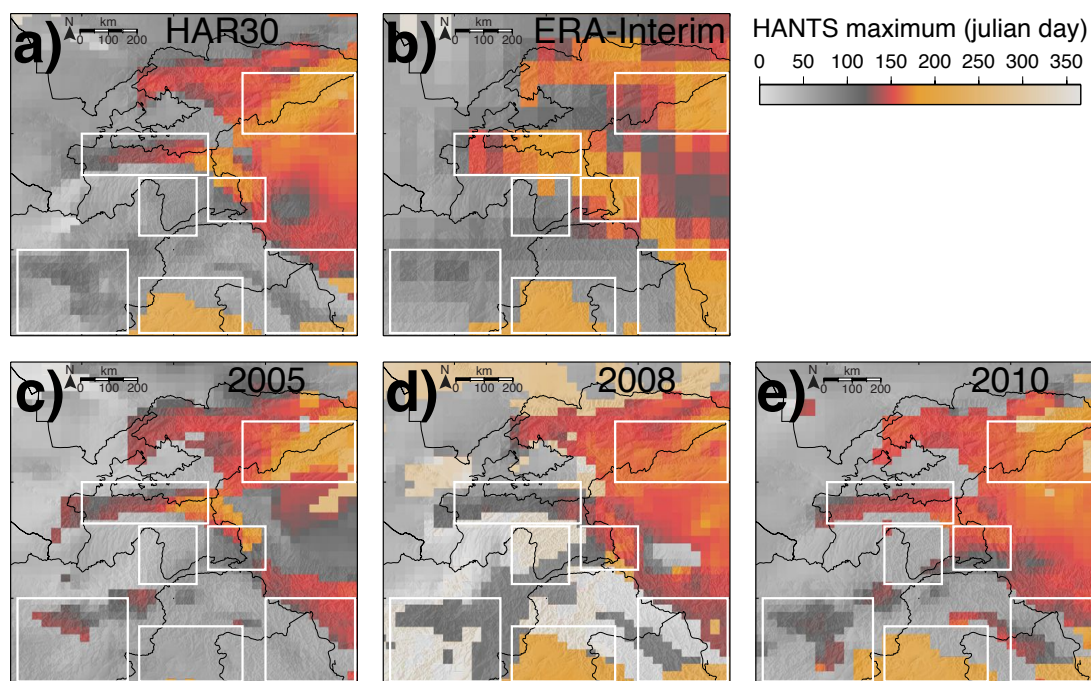


Figure 5. HANTS timing results for (a) the 12-year period of HAR30 and (b) the 35-year period of ERA-Interim for comparison. Timing results for the individually-analyzed years (c) 2005, (d) 2008 and (e) 2010. White bounding boxes correspond to subdivided study sites from Figure 1.

Figure 6 shows the combined meteorological parameters for the individual study sites. All but LWET show very high and rather unsystematic variabilities. LWET in contrast shows high variability between individual years, but intra-annual variabilities are rather weak compared to other parameters. Several study sites display similar temperature anomalies, but show huge differences in precipitation, snow cover and LWET. No causative relationship between individual parameters are immediately apparent,

but individual years show combinations of different mechanisms that lead to specific LWET anomalies. To highlight the relationship of meteorological parameters and LWET anomalies, we exemplarily chose and analyze the three years 2005, 2008 and 2010. These years show very pronounced and different interactions of meteorological parameters. Therefore, they provide the opportunity to systematically describe dominant processes, point out regional differences and describe specific interrelations between meteorological conditions, hydrology and hazards.

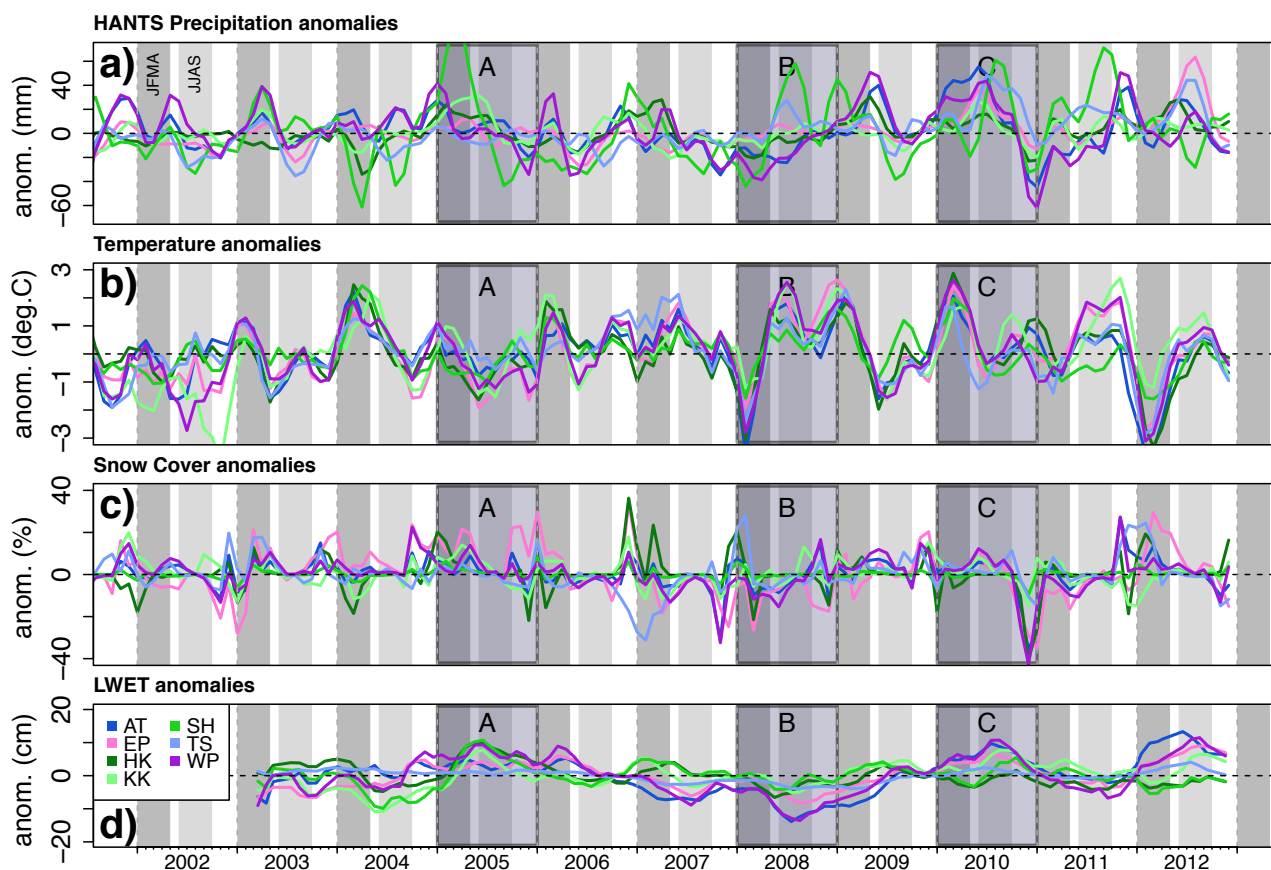


Figure 6. Monthly meteorological anomalies for (a) HANTS precipitation, (b) temperature, (c) snow cover and (d) liquid water equivalent thickness (LWET). The running mean of three months is applied for clearer visualization. Capital letters A, B and C are the three individual years that are analyzed in detail to point out the interplay between meteorological parameters. Vertical dark grey bars denote the winter (JFMA; January–April) and light grey bars the summer (JJAS; June–September) season.

5.2. Individual Years

Figure 7 displays that in 2005 the central and northern sites show only small anomalies for precipitation, while the southern sites, especially SH, show very high winter precipitation. In summer, SH shows reversed, negative precipitation anomalies. A very pronounced negative temperature anomaly in the snow melting season (AMJJA; April–August) (Figure 6b) for the central and southern sites is accompanied by a high snow cover (Figures 6c and 7d). The prevented snow melt correlates with strong positive LWET anomalies (Figure 6d). By September, temperature and snow cover anomalies have

declined. LWET anomalies for the southern sites and WP strongly decline after temperature anomalies become less negative. Reported floods in Tajikistan in June and July, in Afghanistan in June and in Pakistan in June and July (Table 1) coincide with the reduction in snow cover and temperature anomalies. Timings of peak precipitation input show that the usually summer-dominated parts of SH and KK are winter dominated. The central and northern Pamir sites show a picture similar to the average pattern, contrasting the southern Pamir sites (Figure 5c). Spots along the Hindu Kush syntaxis show slightly later peak inputs.

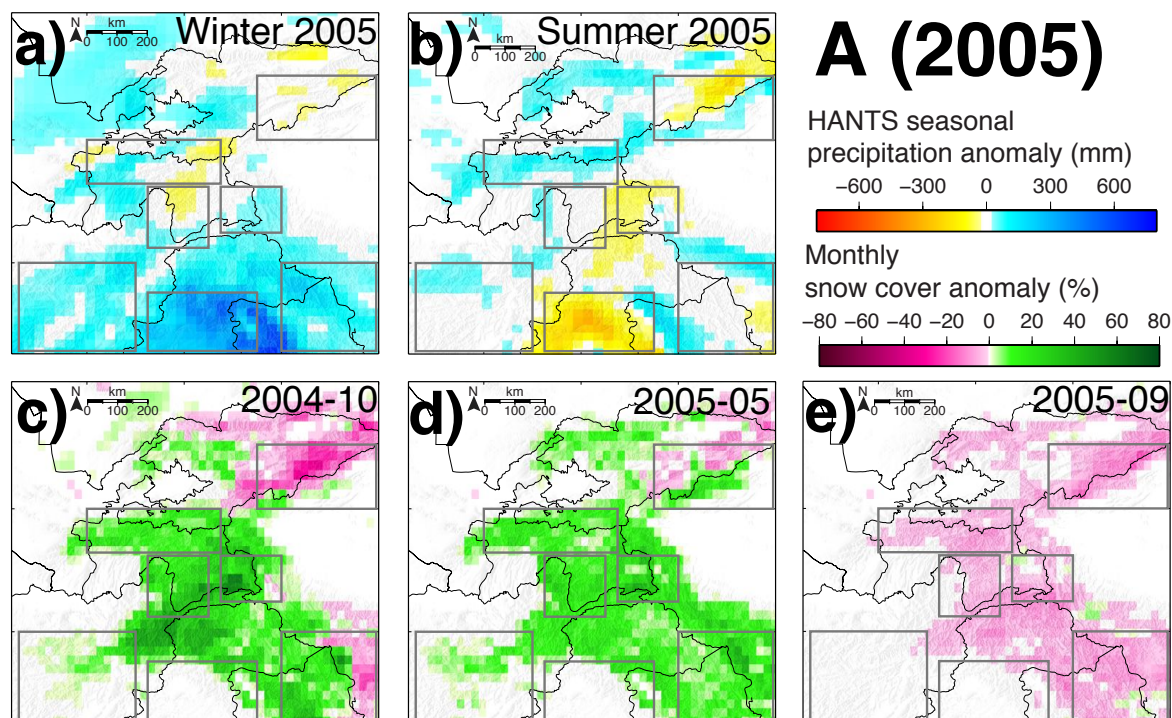


Figure 7. 2005 HANTS precipitation pattern for (a) winter and (b) summer. Very early snow cover in (c) October 2004 lasted till the end of (d) spring 2005 before diminution of snow cover to normal values occurred (see Figure 6), leading to slightly negative anomalies in (e) September 2005.

The year 2008 (Figure 8) is characterized by negative winter precipitation anomalies at all sites. In summer, SH solely shows strong positive anomalies. Western sites show negative anomalies and eastern sites positive ones. Positive temperature anomalies start in May and are most pronounced in July, concentrated in the central Pamirs and the Karakorum Range, where the most extensive glacier cover is present (see Figure 1). Negative anomalies for LWET and positive ones for temperature decline synchronously in summer. The strongest LWET anomalies are evident for AL and WP, which also show the most pronounced negative precipitation anomalies in both winter and summer. Heavy droughts are reported for October in Tajikistan and Afghanistan [53,54], along with two flood events in August for Pakistan (Table 1). Earlier timings of peak precipitation are apparent in the western sites, while summer-dominated regions in the southern parts of SH and KK match the timing of the average pattern (Figure 5d). Slightly earlier peak precipitation occurrence in the most western parts contrasts later

occurrence along the Hindu Kush syntaxis and the EP site. The AL site, despite showing later occurrence than the average pattern, also stands out from the surrounding areas with later occurrences.

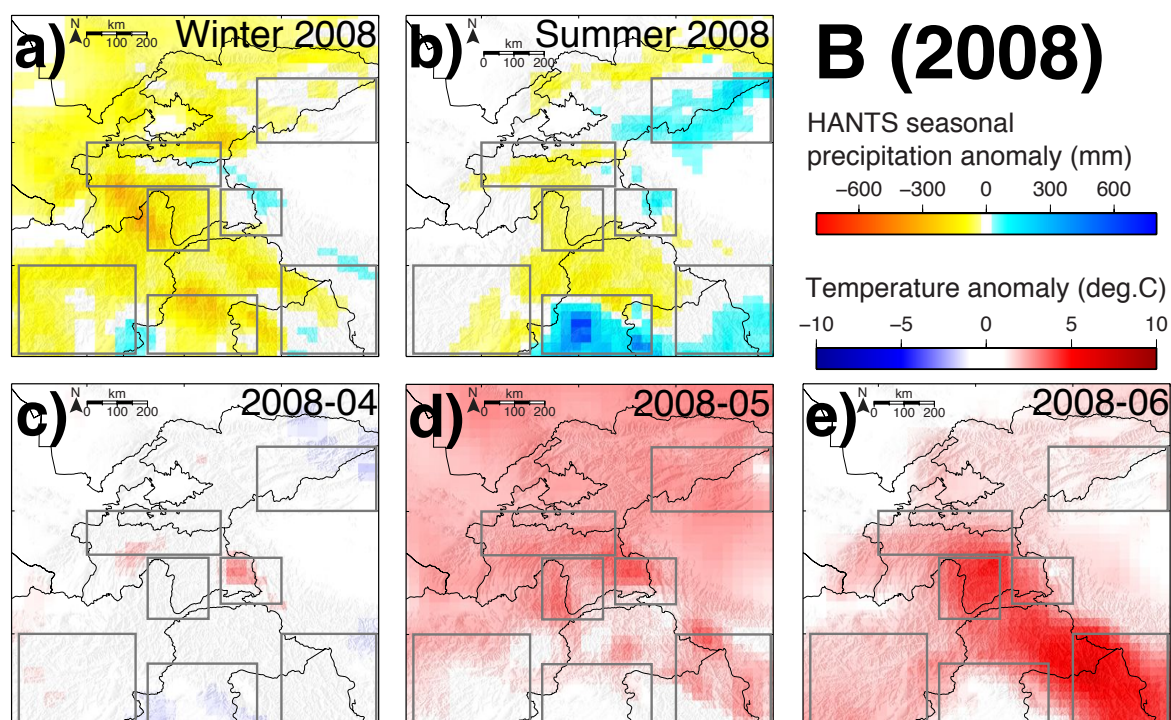


Figure 8. 2008 HANTS precipitation pattern for (a) winter and (b) summer. Gradually-evolving temperature anomalies (c–e) with a concentration of high temperatures at high altitude in the WP, EP and KK sites at the end.

The year 2010 stands out because both summer and winter precipitation anomalies are strongly positive (Figure 9). It also marks the second wettest recorded monsoon year for Pakistan [55]. Especially SH and TS received more precipitation than usual in summer. In winter, the northern and central sites already show positive anomalies that are most pronounced in the AL and WP sites. Strong positive temperature anomalies in winter are not reflected by negative snow cover anomalies. Striking is that the strong June precipitation anomaly coincides with strong positive snow cover anomalies in the central Pamirs, northern Hindu Kush and Karakoram region. By October and later into the year, strong negative precipitation and snow cover anomalies are apparent. This coincides with a leveling out of high positive LWET anomalies. The timing of the Pakistan flood in July/August (e.g., [56]) (Table 1) correlates with the peak of precipitation anomalies for SH. Neither temperature nor snow cover show any anomalies that might be associated with this event. Tajikistan and Afghanistan also encountered flood events that were, however, much earlier in the beginning of May. These events coincide with the strong positive precipitation anomalies in the AL and WP sites starting in winter and continuing into mid-summer, as well as with the still positive temperature anomalies in April and May. Peak precipitation timings show similar timings to the average pattern, but transitional regions in the AL and TS sites show a more discriminated pattern. Along the Hindu Kush syntaxis into the EP site, local spots of later timings are apparent as in 2005, but their spatial extent is more pronounced, almost connecting the HK and

EP sites. Summer-dominated regions in the SH and KK site are also slightly expanded compared to the average pattern.

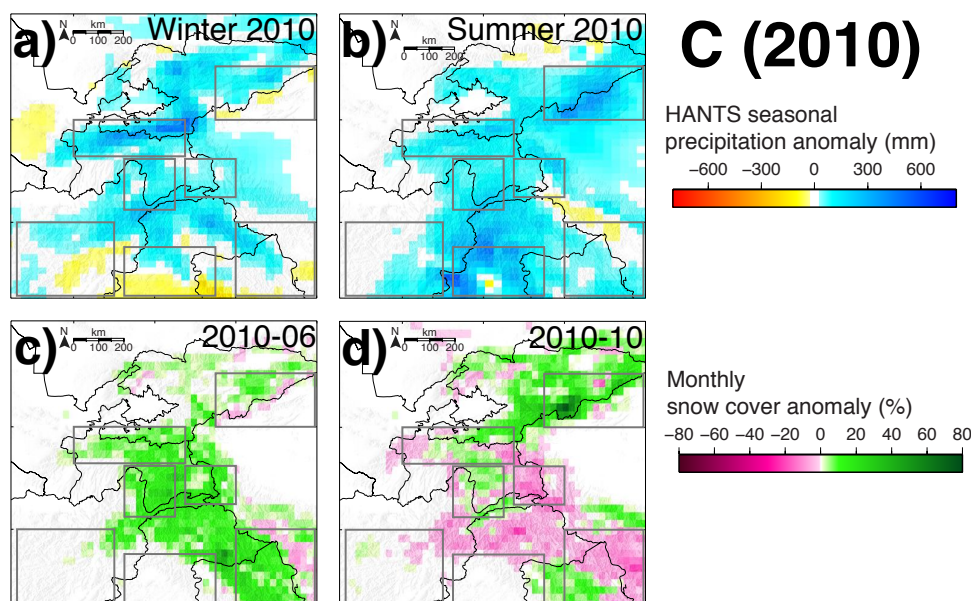


Figure 9. 2010 HANTS precipitation pattern for (a) winter and (b) summer. Strong positive summer precipitation anomalies accompanied by area-wide positive snow cover anomalies for high elevation sites in (c) June 2010. Diminution of snow cover except for TS until (d) the end of summer.

5.3. Spatial Correlation of Winter and Summer Precipitation

Summer and winter anomalies for precipitation and snow cover were used to reveal similar behavior between individual sites and to highlight possible relations of strong/weak summer and winter precipitation anomalies (Figure 10). Significant correlations (p -value < 0.05) are primarily apparent between either winter or summer anomalies of individual sites. In winter, the northern and north-western sites WP, TS and AL show a similar behavior. In the south, SH shows the highest correlation with KK and HK. In summer, WP also correlates with EP and HK, while SH no longer shows significant correlation with any other site.

Comparison of winter and summer anomalies only shows a significant positive correlation for AL. The lowest correlations (≤ 0.25) can be seen for SH and TS. Although other correlations appear non-significant, no negative correlations are found that would suggest an antagonistic relationship between winter and summer precipitation. Comparison of winter or summer precipitation with summer snow cover suggests that AL, WP and EP winter anomalies are related to observed summer snow cover. This relation also holds true for summer precipitation, suggesting that precipitation in both summer and winter contributes to snow cover and partial water storage.

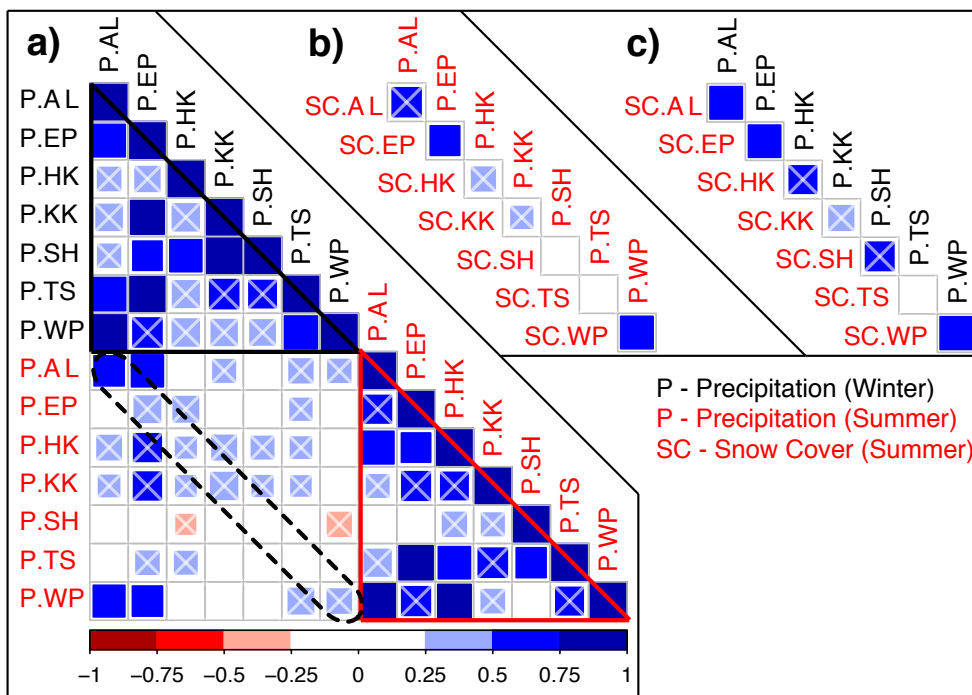


Figure 10. Spatiotemporal correlation of (a) HANTS summer and winter precipitation anomalies; (b) HANTS summer precipitation anomalies with snow cover anomalies; and (c) HANTS winter precipitation anomalies and summer snow cover anomalies. Color coding corresponds to the correlation coefficient multiplied by either one (positive) or -1 (negative correlation). Crosses mark non-significant correlations (p -value ≥ 0.05).

6. Discussion

6.1. HANTS Precipitation and Interplay of Atmospheric Circulations

There are clearly winter and summer precipitation-dominated regions within the greater Pamirs. For both the average and for individual years, this discrimination is most pronounced in the SH and KK sites, as is revealed by the HANTS maxima of the respective time series. The resulting line in the southern Pamirs can be seen as the border of mainly Westerlies- or ISM-dominated regions. The border shows variable locations for individual years and seems (for ISM-dominated precipitation) to be limited by the orographic barrier of the Hindu Kush. Strong winter precipitation in combination with little summer precipitation as, e.g., in 2005 leads to a disappearance of this discrimination line in the study area. Opposite conditions, with stronger summer and weaker winter precipitation, only expand the summer-dominated region by a relatively small portion (2008, 2010), still showing winter dominance along the Hindu Kush syntaxis into the WP and EP sites.

The north-eastern sites TS, AL and EP show especially high variability in peak precipitation timing. The Alay Range shows later timings than the surrounding regions. Aizen *et al.* [4] have pointed out that the northern regions of the Pamirs, including the AL and TS sites, receive a high portion of recycled water during the warm season transferred by northern intrusions. Based on deuterium excess values of sampled snow/ice cores, Aizen *et al.* [4] discriminate the Pamirs (Fedchenko Glacier within the

AL site) to receive either more slowly evaporated or less often evaporated water than the Tian Shan. This differentiation qualitatively follows the presented differences in peak precipitation timing under the assumption that summer precipitation undergoes more recycling than winter precipitation in this area. Although HAR30 precipitation is available for only 12 years, it shows comparable results to 35 years of ERA-Interim precipitation in terms of spatiotemporal distribution as presented by peak precipitation input. This is quite remarkable considering the high weather variability (*cf.* [57]). The obtained spatiotemporal precipitation patterns in the Central Pamirs corroborate a reported strong negative W-E precipitation gradient and later peak precipitation timings in the eastern Pamirs [1]. Because the spatial coverage of rain gauges is sparse in the greater Pamir region, there is no possibility to comprehensively validate the HANTS results. A meaningful comparison with *in situ* data is furthermore impeded by the point-wise character of precipitation gauges that are strongly biased compared to gridded data in mountainous regions. This is due to different orographic effects, such as precipitation shadows and precipitation-altitude gradients. No significant correlations of winter and summer precipitation are apparent for individual sites, except for AL (Figure 10). Most correlations, including correlations between different sites, are positive, but insignificant. Observed strong correlations between different sites in either season show a similarity that might be related to prevailing winds and associated moisture transport.

6.2. Inter-Annual Weather Variability

The three selected years 2005, 2008 and 2010 show very different meteorological settings, allowing one to investigate their effects on the water budget. Although timings of abrupt LWET anomaly changes coincide with major hazard events, the lack of precise hazard locations prevents a derivation of causalities with certainty. The year 2005 illustrates the effect of temperature anomalies on existing snow cover. Especially for high altitude regions (excluding SH), winter precipitation plays a crucial role in different ways. Low temperatures in the preceding year 2004 caused high amounts of precipitation to be stored as snow (Figures 6b–d and 7c). This snow cover persisted late into 2005 due to low temperatures in late spring and summer 2005 (Figure 6b). Even though there are no especially high anomalies in precipitation, this situation favored positive LWET anomalies. The subsequent rapid decline in LWET anomalies suggests high amounts of snow melt. This highlights the strong impact of positive temperature anomalies on the mobilization of large quantities in water. The timing coincides with the occurrence of floods. The role of the high mountains in Central Asia as water towers for the downstream regions [13,58] point to a possible relationship of such melting events and their impact on flooding. However, initially positive precipitation anomalies for the southern sites HK, SH and KK (Figure 6a) equivocally coincide with the timing of flood events. This points to a possible synergetic effect on runoff by (1) increasing temperatures and resulting snowmelt and (2) increased snowmelt from liquid precipitation on top of the snow layer [59].

Different from 2005, 2008 had strong negative winter precipitation anomalies. LWET anomalies reveal that there was slightly less water stored during winter 2008 than usual. Again, positive temperature anomalies in late spring and early summer caused a further decrease in LWET. Negative snow cover and winter precipitation anomalies indicate that snow stocks during early 2008 were already very

low. Snow cover in the Central Pamirs disappears on average by June/July [1,5]. This might have caused strongly increased glacier melt. This assumption is further strengthened by the observed concentrated positive temperature anomalies at high altitudes where the glaciers are located (Figure 1). Pohl *et al.* [1] previously have shown that about 30% of the central Pamirs' annual discharge results from glacier melt. The remaining 70% of annual discharge result almost entirely from snowmelt that also replenishes the groundwater reservoirs. The reduced groundwater discharge and low total amounts of glacier melt, hence, suggest reduced overall river discharge. Again, the role of Central Asia's high mountains as water towers point to reduced river discharge in the mountain foreland regions in summer. The strong arid, continental climate in these regions make river discharge the essential source of irrigation water [13] (Figure 4c), and hence, the occurrence of droughts and reduced stream flow generation in the mountains in Tajikistan and Afghanistan seem to be closely related. At the same time, positive precipitation anomalies in the SH site have caused flood events in the Peshawar district, Pakistan (within the SH site) [60], highlighting the high spatial meteorological variability.

In 2010, the effects of the strong precipitation anomalies are more straight-forward. The high amount of water input is directly reflected by positive LWET anomalies. The southern sites KK and SH that show only small precipitation anomalies in winter show accordingly less LWET. Precipitation in Tajikistan is concentrated in winter and at a high elevation (Figure 4b). Hence, positive winter precipitation anomalies are likely to result in increased snow stocks, without a noticeable effect on winter river discharge [1,5]. The positive temperature anomalies in the winter season are unlikely to affect snowmelt in high mountains, because winter temperatures are well below the dew point [1]. For intermediate elevations, however, temperature anomalies of up to 3°C in combination with high snow stocks and/or increased portions of rainfall over snowfall might result in increased runoff, similar to the effect described for 2005.

These conditions might have led to the reported flood events in Tajikistan and Afghanistan in late spring. Different from that, the severe flood in Pakistan at the end of July 2010 is well documented. Extensive precipitation with high intensities provided moisture to the entire northern regions of Pakistan [56]. Striking is the strong increase of snow cover in June in the high altitude regions all over the Pamirs and the Karakorum Range (Figure 9). This shows that summer precipitation accompanied by normal temperatures for this time can result in significant amounts of precipitation received as snow. Compared to a more immediate response of discharge to rainfall, the response to snowfall is more intermediate, and water is released successively, which weakens the intensity of floods. The delayed release of snowmelt allows for infiltration of water into shallow and subjacent deep groundwater aquifers that buffer regional discharge and provide sustainable groundwater discharge (see LWET) in winter. Such events might further preserve glaciers due to the increased albedo of fresh snow in the early ISM period in June [20,61].

6.3. Impacts on Glacier Evolution

There are only a few studies that have assessed glacier mass balances in the greater Pamir region. Two studies by Gardelle *et al.* [18] and Gardelle *et al.* [19] use a geodetic method that calculates the difference of digital elevation models obtained in two different years (e.g., 1998 and 2010). They show

that the Pamir and Karakorum regions show slightly positive glacier mass balances for the first decade of the 21st century (slightly alternating time periods between the sites). Given the strong inter-annual and intra-annual variability of weather that is presented in this study, one could also assume different outcomes of glacier mass balance studies based on the actual time period that is considered. Moreover, Mölg *et al.* [20] have shown that the Indian monsoon onset timing has a high impact on glacier mass balance in the Tibetan Plateau, because the reflective properties of such precipitation received as snow early in the monsoon season attenuate melting. This highlights the two important aspects of precipitation: (1) providing moisture to accumulate on glaciers; and (2) protecting properties of fresh snow against melting. Furthermore, Liu *et al.* [62] and Khromova *et al.* [63] have pointed out that regional temperature variability plays a key role in glacier retreat at Muztag Ata, eastern Pamir. All of these findings combined highlight that years such as 2008, with negative winter and summer precipitation anomalies, strong positive summer temperature anomalies concentrated at high altitude glacier regions, might have the strongest impacts on glacier retreat. However, it also points out that if glacier evolution studies are based on only two points in time (e.g., Gardelle *et al.* [18], Gardelle *et al.* [19]), they might actually be strongly influenced by the inter-annual variability rather than a persisting trend. Glaciers as a whole feature a response to climate/weather integrated over a spatial area and over a much longer time than, e.g., river discharge or LWET. It would therefore be highly beneficial for the scientific community to investigate short-term responses of glaciers to weather, e.g., how special weather conditions (such as 2008 or 2010) quantitatively affect glacier evolution. The presented timing maps of peak precipitation input could be used as indicators, where such measurements would yield the most valuable insights. The strong spatiotemporal variability of glacial advances in the Quaternary across the greater Pamir region [2] does not provide a picture as consistent as the presented timing maps of peak precipitation input. This is to a large degree due to the very limited amount of available studies, which prevents any meaningful analysis at this moment. However, our results can help to develop sampling strategies for such studies and, thus, help to relate past and present-day climate and their effects on glacier evolution.

6.4. Impacts on Hazards

We demonstrated the qualitative agreement of meteorological and hydrological anomalies and their described interplay with hazard events. Hazard events are reported at the country scale and, thus, prevent deriving causalities with certitude. However, rivers of Central Asia originate in the high mountains [13,58], and therefore, strong floods and/or droughts are bound to hydrological conditions in the mountains. This gives reason to imply a causal link even at the country scale. The derived insights into mechanisms that can lead to hazardous events can help to complement more geomorphologic and static hazard potential studies (e.g., Gruber and Mergili [64]), which disregard quickly changing meteorological parameters. Integration of such studies with our approach could help to get a more complementary approach that transitions from general risk potential (based on geomorphology and long-term meteorological/climate conditions) into acute risks resulting from short-term weather patterns. A major limitation is the lack of real-time RCM data, allowing only post analysis with the selected datasets. The presented maps of precipitation anomalies, however, reveal similarities in precipitation for several regions that could provide feasible locations for future

precipitation and temperature gauges in the scarcely-monitored Pamirs. Due to the similarity in temperature anomalies between the study sites (Figure 6b), the few available meteorological stations might already provide sufficient information to infer strong melting events that can result in floods. Remote sensing precipitation products are not feasible for this approach at the moment due to issues with detecting snowfall and/or very low precipitation intensities [11,12], especially in mountainous regions. The recently launched Global Precipitation Measurement mission (GPM) [65] might close this gap and allow analysis with little time delay. Even until then, LWET anomalies from GRACE data provide high explanatory power for quick hazard identification, especially for spring and summer flood assessments. This is due to the temporal decoupling of snow accumulation in winter and the release of water in spring and summer, allowing a certain time lag between observation and compilation of the dataset. Even one-month delayed data could provide the essential LWET values that can be used for the assessment of a potential water release. Remote sensing products to capture land surface temperatures, which have been shown to be a reliable proxy for near surface air temperatures [1], such as MODIS MOD11, can then be utilized to quickly issue warnings if positive temperature anomalies and, hence, strong meltings are expected.

7. Conclusions

We present a multi-source approach based on climate model data and remote sensing products to highlight the effects of winter and summer precipitation anomalies on the greater Pamirs. We use an in-house developed toolbox of HANTS that explores seasonal patterns in time series of gridded datasets, such as remote sensing or climate model data. We incorporate independent remote sensing-based datasets of snow cover (MODIS) and liquid water equivalent thicknesses (GRACE), along with RCM data for temperature and precipitation. Anomalies of precipitation, temperature, snow cover and LWET reveal different interplays of meteorological parameters. We select three characteristic climatic situations to exemplify the complex climatic feedbacks. This consistency is further highlighted by the qualitative agreement of water mobilization or lack thereof, with droughts and floods. Probably because of issues related to snowfall detection, we had to discard remotely-sensed precipitation data that are still not a reliable input parameter in mountainous areas. Hence, we rely on the best performing precipitation dataset for this region, HAR30. The near future will hopefully provide promising alternatives to RCM data, e.g., with the Global Precipitation Measurement (GPM) datasets, allowing one to directly incorporate remote sensing data with little time delay from acquisition to application. The GRACE and MODIS remote sensing data proved to be useful additional material to corroborate HANTS analysis and to provide supplementary information to infer the underlying processes.

By applying the HANTS algorithm, we were able to investigate precipitation time series that show high variability and are difficult to investigate using simple averaging or smoothing methods. We define distinct regions of summer and winter dominance surrounding intermediate regions. This quantitative approach allows us to refine the previous vague characterization of the Pamirs as a transition zone between Westerlies and the ISM to a now spatially more precise distinction of individual regions as winter-, summer- or transitionally-dominated. Anomalies inter-comparison of (1) precipitation, (2) temperature, (3) snow cover and (4) LWET display high consistency and highlight the complex

processes that affect hydrology, glacier evolution and hazard potentials in the high mountains of Central Asia. We do not find any significant indications for causal summer and winter precipitation interactions. Instead, high variability of either meteorological component results in the specific scenarios that are presented and discussed. We find that temperature in combination with (without) snow cover has high impacts on the change in LWET. Consequently, this must correspond to varying streamflow and, thus, the occurrence of floods (droughts). Especially in the high mountain regions, positive precipitation anomalies result in large snow stocks that, depending on temperature anomalies, can quickly release high amounts of melt water, barring the risk of floods. However, the strongly heterogeneous distribution of precipitation might cause local floods, while only a few hundred kilometers away, severe droughts occur. The presented approach and delineated regions of summer, winter and transitional dominance might help to provide a valuable basis for glaciological, hydrological, but also paleoclimatological studies that often struggle to refer to certain moisture transport systems. The open access HANTS toolbox promises to be an efficient tool to explore the spatiotemporal variability of cyclic signals in remote sensing data.

Acknowledgments

This work is part of the BMBF (Bundesministerium für Bildung und Forschung; German Federal Ministry of Education and Research) research program PAMIR (Impact of climate change on the water balance of a river basin in the Pamir) (funding code: FKZ 03G0815) within the CAME (Central Asia and Tibet: Monsoon dynamics and geo-ecosystems) project and funded by the BMBF. MODIS MCD12Q1 data are distributed by the Land Processes Distributed Active Archive Center (LP DAAC), located at the U.S. Geological Survey (USGS) Earth Resources Observation and Science (EROS) Center (lpdaac.usgs.gov). GRACE land data were processed by Sean Swenson, supported by the NASA MEaSUREs (Making Earth System Data Records for Use in Research Environments) Program, and are available at <http://grace.jpl.nasa.gov>. Generic Mapping Tools (GMT) <http://gmt.soest.hawaii.edu/> were used to produce the maps. We would like to thank four anonymous reviewers for their comments, which helped to improve this manuscript. We further like to thank the editorial board for their guidance and decisions made in the review process. Processing and analyzing of the data were conducted with the aid of the statistical software R [66], including the packages “raster” [67] and “rgdal” [68]. The PAMIR team further includes Malte Knoche, Christiane Meier, Stephan Weise, Karsten Osenbrück, Stefan Geyer, Tino Rödiger, Christian Siebert and Wolfgang Busch.

Author Contributions

All authors conceptualized the manuscript. Eric Pohl drafted the manuscript, conducted the data extraction, the data processing and the application of the HANTS algorithm. All co-authors guided the application with HANTS and provided revision throughout the study.

Conflicts of Interest

The authors declare no conflict of interest.

References

1. Pohl, E.; Knoche, M.; Gloaguen, R.; Andermann, C.; Krause, P. The hydrological cycle in the high Pamir Mountains: How temperature and seasonal precipitation distribution influence stream flow in the Gunt catchment, Tajikistan. *Earth Surf. Dyn. Discuss.* **2014**, *2*, 1155–1215.
2. Fuchs, M.C.; Gloaguen, R.; Pohl, E. Tectonic and climatic forcing on the Panj river system during the Quaternary. *Int. J. Earth Sci.* **2013**, *102*, 1985–2003.
3. Tahir, A.A.; Chevallier, P.; Arnaud, Y.; Ahmad, B. Snow cover dynamics and hydrological regime of the Hunza River basin, Karakoram Range, Northern Pakistan. *Hydrol. Earth Syst. Sci. Discuss.* **2011**, *8*, 2821–2860.
4. Aizen, V.B.; Mayewski, P.A.; Aizen, E.M.; Joswiak, D.R.; Surazakov, A.B.; Kaspari, S.; Grigholm, B.; Krachler, M.; Handley, M.; Finaev, A. Stable-isotope and trace element time series from Fedchenko glacier (Pamirs) snow/firn cores. *J. Glaciol.* **2009**, *55*, 275–291.
5. Immerzeel, W.; Droogers, P.; de Jong, S.; Bierkens, M. Large-scale monitoring of snow cover and runoff simulation in Himalayan river basins using remote sensing. *Remote Sens. Environ.* **2009**, *113*, 40–49.
6. Lutz, A.F.; Immerzeel, W.W.; Shrestha, A.B.; Bierkens, M.F.P. Consistent increase in High Asia's runoff due to increasing glacier melt and precipitation. *Nat. Clim. Chang.* **2014**, *4*, 587–592.
7. Hagg, W.; Braun, L.; Kuhn, M.; Nesgaard, T. Modelling of hydrological response to climate change in glacierized Central Asian catchments. *J. Hydrol.* **2007**, *332*, 40–53.
8. Sorg, A.; Bolch, T.; Stoffel, M.; Solomina, O.; Beniston, M. Climate change impacts on glaciers and runoff in Tien Shan (Central Asia). *Nat. Clim. Chang.* **2012**, *2*, 725–731.
9. Bookhagen, B.; Burbank, D.W. Toward a complete Himalayan hydrological budget: Spatiotemporal distribution of snowmelt and rainfall and their impact on river discharge. *J. Geophys. Res.* **2010**, *115*, 1–25.
10. Palazzi, E.; Hardenberg, J.V.; Provenzale, A. Precipitation in the Hindu-Kush Karakoram Himalaya: Observations and future scenarios. *J. Geophys. Res.: Atmos.* **2013**, *118*, 85–100.
11. Skofronick-Jackson, G.; Weinman, J. A physical model to determine snowfall over land by microwave radiometry. *IEEE Trans. Geosci. Remote Sens.* **2004**, *42*, 1047–1058.
12. Prigent, C. Precipitation retrieval from space: An overview. *Comptes Rendus Geosci.* **2010**, *342*, 380–389.
13. Unger-Shayesteh, K.; Vorogushyn, S.; Farinotti, D.; Gafurov, A.; Duethmann, D.; Mandychev, A.; Merz, B. What do we know about past changes in the water cycle of Central Asian headwaters? A review. *Glob. Planet. Chang.* **2013**, *110*, 4–25.
14. Zech, R.; Abramowski, U.; Glaser, B.; Sosin, P.; Kubik, P.; Zech, W. Late Quaternary glacial and climate history of the Pamir Mountains derived from cosmogenic be exposure ages. *Quat. Res.* **2005**, *64*, 212–220.
15. Röhringer, I.; Zech, R.; Abramowski, U.; Sosin, P.; Aldahan, A.; Kubik, P.W.; Zöller, L.; Zech, W. The late Pleistocene glaciation in the Bogchigir Valleys (Pamir, Tajikistan) based on ^{10}Be surface exposure dating. *Quat. Res.* **2012**, *78*, 590–597.

16. Seong, Y.B.; Owen, L.a.; Yi, C.; Finkel, R.C. Quaternary glaciation of Muztag Ata and Kongur Shan: Evidence for glacier response to rapid climate changes throughout the Late Glacial and Holocene in westernmost Tibet. *Geol. Soc. Am. Bull.* **2009**, *121*, 348–365.
17. Maussion, F.; Scherer, D.; Mölg, T.; Collier, E.; Curio, J.; Finkelnburg, R. Precipitation seasonality and variability over the Tibetan Plateau as resolved by the High Asia reanalysis. *J. Clim.* **2014**, *27*, 1910–1927.
18. Gardelle, J.; Berthier, E.; Arnaud, Y. Slight mass gain of Karakoram glaciers in the early Twenty-First century. *Nat. Geosci.* **2012**, *5*, 322–325.
19. Gardelle, J.; Berthier, E.; Arnaud, Y.; Kääh, A. Region-wide glacier mass balances over the Pamir-Karakoram-Himalaya during 1999–2011. *Cryosphere* **2013**, *7*, 1263–1286.
20. Mölg, T.; Maussion, F.; Yang, W.; Scherer, D. The footprint of Asian monsoon dynamics in the mass and energy balance of a Tibetan glacier. *Cryosphere* **2012**, *6*, 1445–1461.
21. de Jong, R.; de Bruin, S.; de Wit, A.; Schaepman, M.E.; Dent, D.L. Analysis of monotonic greening and browning trends from global NDVI time-series. *Remote Sens. Environ.* **2011**, *115*, 692–702.
22. Roerink, G.J.; Menenti, M.; Verhoef, W. Reconstructing cloudfree NDVI composites using Fourier analysis of time series. *Int. J. Remote Sens.* **2000**, *21*, 1911–1917.
23. Li, W.; Luo, C.; Wang, D.; Lei, T. Diurnal variations of precipitation over the South China Sea. *Meteorol. Atmos. Phys.* **2010**, *109*, 33–46.
24. Justino, F.; Setzer, A.; Bracegirdle, T.J.; Mendes, D.; Grimm, A.; Dechiche, G.; Schaefer, C.E.G.R. Harmonic analysis of climatological temperature over Antarctica: Present day and greenhouse warming perspectives. *Int. J. Climatol.* **2011**, *31*, 514–530.
25. Xu, Y.; Shen, Y.; Wu, Z. Spatial and temporal variations of land surface temperature over the Tibetan Plateau based on Harmonic analysis. *Mount. Res. Dev.* **2013**, *33*, 85–94.
26. Horn, L.H.; Bryson, R.A. Harmonic analysis of the annual March of precipitation over the United States 1. *Ann. Assoc. Am. Geogr.* **1960**, *50*, 157–171.
27. Kirkyla, K.I.; Hameed, S. Harmonic analysis of the seasonal cycle in precipitation over the United States: A comparison between observations and a general circulation model. *J. Clim.* **1989**, *2*, 1463–1475.
28. Kadioğlu, M.; Öztürk, N.; Erdun, H.; Şen, Z. On the precipitation climatology of Turkey by harmonic analysis. *Int. J. Climatol.* **1999**, *19*, 1717–1728.
29. Tarawneh, Q. Harmonic analysis of precipitation climatology in Saudi Arabia. *Theor. Appl. Climatol.* **2015**.
30. Seiler, R. Analyse linearer Trends in der Phänologie multimodaler Vegetation, Auswertung von NDVI Zeitreihen für das Niger Binnendelta (Rep. Mali / Westafrika) (in German). In Proceedings of the 32nd Scientific–Technical Annual Meeting of the DGPF (Deutsche Gesellschaft für Photogrammetrie, Fernerkundung und Geoinformation e.V.), Potsdam, Germany, 14–17 March 2012; Volume 21, pp. 65–74.
31. Seiler, R.; Gloaguen, R. (Non-)linear phenological trends in an ecosystem with multiple growing seasons derived from AVHRR-NDVI time series. In Proceedings of the 2012 IEEE International Geoscience and Remote Sensing Symposium (IGARSS), Munich, Germany, 22–27 July 2012; pp. 6789–6792.

32. Yao, T.; Thompson, L.; Yang, W.; Yu, W.; Gao, Y.; Guo, X.; Yang, X.; Duan, K.; Zhao, H.; Xu, B.; *et al.* Different glacier status with atmospheric circulations in Tibetan Plateau and surroundings. *Nat. Clim. Chang.* **2012**, *2*, 663–667.
33. Fuchs, M.C.; Gloaguen, R.; Krbetschek, M.; Szulc, A. Rates of river incision across the main tectonic units of the Pamir identified using optically stimulated luminescence dating of fluvial terraces. *Geomorphology* **2014**, *216*, 79–92.
34. Huffman, G.J. Estimates of Root-Mean-Square Random Error for finite samples of estimated precipitation. *J. Appl. Meteorol.* **1997**, *36*, 1191–1201.
35. Huffman, G.J.; Adler, R.F.; Arkin, P.; Chang, A.; Ferraro, R.; Gruber, A.; Janowiak, J.; McNab, A.; Rudolf, B.; Schneider, U. The Global Precipitation Climatology Project (GPCP) combined precipitation dataset. *Bull. Am. Meteorol. Soc.* **1997**, *78*, 5–20.
36. Huffman, G.J.; Adler, R.F.; Bolvin, D.T.; Gu, G.; Nelkin, E.J.; Bowman, K.P.; Hong, Y.; Stocker, E.F.; Wolff, D.B. The TRMM Multisatellite Precipitation Analysis (TMPA): Quasi-global, multiyear, combined-sensor precipitation estimates at fine scales. *J. Hydrometeorol.* **2007**, *8*, 38.
37. Yin, Z.Y. Using a geographic information system to improve Special Sensor Microwave Imager precipitation estimates over the Tibetan Plateau. *J. Geophys. Res.* **2004**, *109*, D03110.
38. Kamal-Heikman, S.; Derry, L.A.; Stedinger, J.R.; Duncan, C.C. A simple predictive tool for lower Brahmaputra River Basin monsoon flooding. *Earth Interact.* **2007**, *11*, 1–11.
39. Prigent, C. Precipitation retrieval from space: An overview. *Comptes Rendus Geosci.* **2010**, *342*, 380–389.
40. Dee, D.P.; Uppala, S.M.; Simmons, A.J.; Berrisford, P.; Poli, P.; Kobayashi, S.; Andrae, U.; Balmaseda, M.A.; Balsamo, G.; Bauer, P.; *et al.* The ERA-Interim reanalysis: Configuration and performance of the data assimilation system. *Q. J. R. Meteorol. Soc.* **2011**, *137*, 553–597.
41. National Centers for Environmental Prediction–NOAA, U.S. Department of Commerce, National Weather Service (NWS). NCEP FNL Operational Model Global Tropospheric Analyses, Continuing from July 1999. Available online: <http://rda.ucar.edu/datasets/ds083.2/#access> (accessed on 10 July 2015).
42. Skamarock, W.C.; Klemp, J.B. A time-split nonhydrostatic atmospheric model for weather research and forecasting applications. *J. Comput. Phys.* **2008**, *227*, 3465–3485.
43. Hall, D.K.; Salomonson, V.V.; Riggs, G.A. *MODIS/Terra Snow Cover Monthly L3 Global 0.05Deg CMG, Version 5. [MOD10CM]*; National Snow and Ice Data Center: Boulder, CO, USA, 2006.
44. Dietz, A.; Conrad, C.; Kuenzer, C.; Gesell, G.; Dech, S. Identifying changing snow cover characteristics in Central Asia between 1986 and 2014 from remote sensing data. *Remote Sens.* **2014**, *6*, 12752–12775.
45. Hall, D.K.; Salomonson, V.V.; Riggs, G.A. *MODIS/Terra Snow Cover Daily L3 Global 0.05deg CMG V005. [MOD10C1]*; National Snow and Ice Data Center: Boulder, CO, USA, 2006.
46. Landerer, F.W.; Swenson, S.C. Accuracy of scaled GRACE terrestrial water storage estimates. *Water Resour. Res.* **2012**, *48*, W04531.
47. Swenson, S.; Wahr, J. Post-processing removal of correlated errors in GRACE data. *Geophys. Res. Lett.* **2006**, *33*, L08402.

48. Dahle, C.; Flechtner, F.; Gruber, C.; König, D.; König, R.; Michalak, G.; Neumayer, K.H. *GFZ GRACE Level-2 Processing Standards Document for Level-2 Product Release 0005: Revised Edition*; Technical Report; Deutsches GeoForschungsZentrum GFZ: Potsdam, Germany, 2013.
49. Lettenmaier, D.P.; Famiglietti, J.S. Hydrology: Water from on high. *Nature* **2006**, *444*, 562–563.
50. Syed, T.H.; Famiglietti, J.S.; Rodell, M.; Chen, J.; Wilson, C.R. Analysis of terrestrial water storage changes from GRACE and GLDAS. *Water Resour. Res.* **2008**, doi:10.1029/2006WR005779.
51. Ramillien, G.; Famiglietti, J.S.; Wahr, J. Detection of continental hydrology and glaciology signals from GRACE: A review. *Surv. Geophys.* **2008**, *29*, 361–374.
52. Jacob, T.; Wahr, J.; Pfeffer, W.T.; Swenson, S. Recent contributions of glaciers and ice caps to sea level rise. *Nature* **2012**, *482*, 514–8.
53. Guha-Sapir, D.; Below, R.; Hoyois, P. *EM-DAT: International Disaster Database*; Technical Report; Université Catholique de Louvain: Brussels, Belgium, 2014.
54. Beekma, J.; Fiddes, J. Floods and droughts : The Afghan water paradox. In *Afghanistan Human Development Report 2011*; Kabul University (UNDP-Afghanistan): Kabul, Afghanistan, 2011; pp. 1–30.
55. Mahmood, A.; Faisal, N.; Jameel, A. *Special Report on Pakistan's Monsoon 2011 Rainfall*; Technical Report January; Pakistan Meteorological Department: Karachi, Pakistan, 2012.
56. Houze, R.A.; Rasmussen, K.L.; Medina, S.; Brodzik, S.R.; Romatschke, U. Anomalous atmospheric events leading to the summer 2010 floods in Pakistan. *Bull. Am. Meteorol. Soc.* **2011**, *92*, 291–298.
57. Kapnick, S.B.; Delworth, T.L.; Ashfaq, M.; Malyshev, S.; Milly, P.C.D. Snowfall less sensitive to warming in Karakoram than in Himalayas due to a unique seasonal cycle. *Nat. Geosci.* **2014**, *7*, 834–840.
58. Immerzeel, W.W.; van Beek, L.P.H.; Bierkens, M.F.P. Climate change will affect the Asian water towers. *Science* **2010**, *328*, 1382–1385.
59. Harr, R.D. Some characteristics and consequences of snowmelt during rainfall in western Oregon. *J. Hydrol.* **1981**, *53*, 277–304.
60. World Health Organization. *Pakistan Floods Situation Report#F-1-2008 (Aug 3–5, 2008)*; Technical Report; World Health Organization–Country Office, National Institute of Health: Islamabad, Pakistan, 2008.
61. Fujita, K.; Ageta, Y. Effect of summer accumulation on glacier mass balance on the Tibetan Plateau revealed by mass-balance model. *J. Glaciol.* **2000**, *46*, 244–252.
62. Liu, X.; Herzschuh, U.; Wang, Y.; Kuhn, G.; Yu, Z. Glacier fluctuations of Muztagh Ata and temperature changes during the late Holocene in westernmost Tibetan Plateau, based on glaciolacustrine sediment records. *Geophys. Res. Lett.* **2014**, *41*, 6265–6273.
63. Khromova, T.; Osipova, G.; Tsvetkov, D.; Dyurgerov, M.; Barry, R. Changes in glacier extent in the eastern Pamir, Central Asia, determined from historical data and ASTER imagery. *Remote Sens. Environ.* **2006**, *102*, 24–32.
64. Gruber, F.E.; Mergili, M. Regional-scale analysis of high-mountain multi-hazard and risk indicators in the Pamir (Tajikistan) with GRASS GIS. *Nat. Hazards Earth Syst. Sci.* **2013**, *13*, 2779–2796.

65. Hou, A.Y.; Kakar, R.K.; Neeck, S.; Azarbarzin, A.A.; Kummerow, C.D.; Kojima, M.; Oki, R.; Nakamura, K.; Iguchi, T. The Global Precipitation Measurement Mission. *Bull. Am. Meteorol. Soc.* **2014**, *95*, 701–722.
66. R Core Team. *R: A Language and Environment for Statistical Computing*; R Foundation for Statistical Computing: Vienna, Austria, 2014.
67. Hijmans, R.J. raster: Geographic Data Analysis and Modeling, 2015; R Package Version 2.4-15. Available online: <http://CRAN.R-project.org/package=raster> (accessed on 29 July 2015).
68. Bivand, R.; Keitt, T.; Rowlingson, B. rgdal: Bindings for the Geospatial Data Abstraction Library, 2015; R Package Version 1.0-4. Available online: <http://CRAN.R-project.org/package=rgdal> (accessed on 29 July 2015).

© 2015 by the authors; licensee MDPI, Basel, Switzerland. This article is an open access article distributed under the terms and conditions of the Creative Commons Attribution license (<http://creativecommons.org/licenses/by/4.0/>).